Draft version December 11, 2017
Typeset using LaTeX **twocolumn** style in AASTeX61

NO TIME FOR DEAD TIME - USE THE FOURIER AMPLITUDE DIFFERENCES TO NORMALIZE DEAD TIME-AFFECTED PERIODOGRAMS

Matteo Bachetti[1] and Daniela Huppenkothen[2,3]

[1] *INAF-Osservatorio Astronomico di Cagliari, via della Scienza 5, I-09047 Selargius (CA)*
[2] *Center for Data Science, New York University, 60 5h Avenue, 7th Floor, New York, NY 10003*
[3] *Center for Cosmology and Particle Physics, Department of Physics, New York University, 4 Washington Place, New York, NY 10003, USA*

(Received XXXX; Revised XXXX; Accepted December 11, 2017)

Submitted to ApJL

ABSTRACT

Dead time affects many of the instruments used in X-ray astronomy, by producing a strong distortion in power density spectra. This can make it difficult to model the aperiodic variability of the source or look for quasi-periodic oscillations. Whereas in some instruments a simple a-priori correction for dead time-affected power spectra is possible, this is not the case for others such as *NuSTAR*, where the dead time is non-constant and long ($\sim$2.5 ms). Bachetti et al. (2015) suggested the cospectrum obtained from light curves of independent detectors within the same instrument as a possible way out, but this solution has always only been a partial one: the measured r.m.s. was still affected by dead time, because the width of the power distribution of the cospectrum was modulated by dead time in a frequency-dependent way.

In this Letter we suggest a new, powerful method to normalize deadtime-affected cospectra and power density spectra. Our approach uses the difference of the Fourier amplitudes from two independent detectors to characterize and filter out the effect of dead time. This method is crucially important for the accurate modeling of periodograms derived from instruments affected by dead time on board current missions like *NuSTAR* and *Astrosat*, but also future missions such as *IXPE*.

Keywords: X-rays: binaries — X-rays: general — methods: data analysis — methods: statistical

Corresponding author: Matteo Bachetti
bachetti@oa-cagliari.inaf.it

1. INTRODUCTION

Dead time is an unavoidable and common issue of photon-counting instruments. It is the time t_d that the instrument takes to process an event and be ready for the next event. In most current astronomical photon-counting X-ray missions, dead time is of the *non-paralyzable* kind, meaning that the instrument does not accept new events during dead time, avoiding a complete lock of the instrument if the incident rate of photons is higher than $1/t_d$. Being roughly energy-independent, dead time is not usually an issue for spectroscopy, as it only affects the maximum rate of photons that can be recorded, so it basically only increases the observing time needed for high quality spectra. For timing analysis, the effect of dead time is far more problematic. The periodogram, commonly referred to as power density spectrum (PDS)[1], which is the most widely used statistical tool to investigate rapid variability, is heavily distorted by dead time, with a characteristic pattern similar to a damped oscillator. This pattern is stronger for brighter sources, and it is often not possible to disentangle this power spectral distortion due to dead time and the broadband noise components characterizing the emission of accreting systems. In the special case where dead time is constant, its shape can be modeled precisely (Zhang et al. 1995; Vikhlinin et al. 1994). However, dead time is often different on an event-to-event basis, and it is not obvious how to model it precisely, also because the information on dead time is often incomplete in the data files distributed by HEASARC[2]. For a more thorough discussion about different dead time behaviors see Zhang et al. (1995).

When using data from missions carrying two or more *identical and independent* detectors like *NuSTAR*, Bachetti et al. (2015) proposed an approach to mitigate instrumental effects like dead time exploiting this redundancy: where in standard analysis, light curves of multiple detectors are summed before Fourier transforming the summed light curve, it is possible to instead Fourier-transform the signal of two independent detectors and combine the Fourier amplitudes in a *cospectrum* – the real part of the cross spectrum – instead of the periodogram. Since dead time is uncorrelated between the two detectors, the resulting powers have a mean white noise level fixed to 0, which resolves the first and most problematic issue created by dead time (see details in Bachetti et al. 2015); however, the resulting powers no longer follow the statistical distribution expected for power spectra, and their probability distribution is frequency-dependent. Whereas a noise cospectrum in the absence of dead time would follow a Laplace distribution (Huppenkothen and Bachetti, sub.), dead time affects the width of the probability distribution for cospectral powers and modulates the measured r.m.s. proportionally to the distortion acted on power spectra. In this Letter, we show a method to precisely recover the shape of the power density spectrum by looking at the difference of the Fourier amplitudes of the light curves of two independent detectors. This difference, in fact, contains information on the uncorrelated noise produced by dead time, but not on the source-related signal which is correlated between the two detectors. This allows to disentangle the effects of dead time from those of the source variability.

In Section 2 we briefly describe our data analysis and simulation setup. In Section 3 we show that, in the absence of dead time, the Fourier amplitudes of two independent detectors contain the sum of the correlated signal (the source signal) and uncorrelated noise (detector-related noise), and that their difference eliminates the source part. In Section 4 we show that, in the presence of dead time, the difference of the Fourier amplitude still eliminates the source signal but retains information on dead time effects. In Section 6 we show that this can be used to recover the dead noise-free power spectrum.

2. DATA SIMULATION

All simulated and real data sets in this paper were produced and/or analyzed with a combination of the two Python libraries `stingray`[3] (Huppenkothen et al. 2016) and `HENDRICS` v.3.0b2 (formerly known as MaLTPyNT; Bachetti 2015), both based on Astropy (Astropy Collaboration et al. 2013).

We used the same procedure and algorithms described by Bachetti et al. (2015), Section 4, that we briefly recall here together with references to the methods and classes of the libraries above where these steps are implemented. We used the Timmer & Koenig (1995) method to create a noise-affected light curve starting from a given power spectral shape. This method is implemented in the `stingray.simulate` module. This step needs to be done carefully: if the initial light curves contain signifi-

[1] here we will use the term PDS for the actual source power spectrum, and *periodogram* to indicate our estimate of it, or otherwise said, the realization of the "real" power spectrum we observe in the data

[2] Whereas in principle this information could be obtained by using the PRIOR column in the unfiltered event files for some missions, the live time given in this column is affected by events that are not recorded in the file, like shield vetos in the case of *NuSTAR*, and the estimate of dead time is necessarily uncertain

[3] The library is under heavy development. For this work we used the version identified by the hash `3e64f3d`

cant random noise, the process for the creation of events creates a random variate on the top of the local count rate - which is varying randomly already - producing a non-Poissonian final light curve. So, we initially simulated light curves with a very high "count rate" - so that the Poisson noise was relatively small - then renormalized the light curves to the wanted (lower) count rate and r.m.s. and finally used these light curves to simulate event lists using the rejection sampling, implemented in the `stingray.Eventlist.simulate_times()` method. Finally, the `hendrics.fake.filter_for_deadtime()` function was used to apply a non-paralyzable dead time of 2.5 ms to the simulated event lists. For more details on the simulated data sets, see also Section 6 and the available Jupyter notebooks[4] (for a description of Jupyter notebooks, see Kluyver et al. 2016).

3. ON THE DIFFERENCE OF FOURIER AMPLITUDES

Let us consider two identical and independent detectors observing the same variable source, producing independent and strictly simultaneous time series, with identical binning, $\mathbf{x} = \{x_k\}_{k=1}^N$ and $\mathbf{y} = \{y_k\}_{k=1}^N$. For a stochastic process (e.g. $1/\nu$-type red noise), the Fourier amplitudes will vary as a function of $N_{\rm phot}P(\nu)/4$, where $P(\nu)$ is the shape of the power spectrum underlying the stochastic process, and $N_{\rm phot}$ denotes the number of photons in a light curve. If the two detectors observe the same source simultaneously, the amplitudes and phases of the stochastic process will be shared among $\mathbf{x}$ and $\mathbf{y}$, while each light curve will be affected *independently* by both the photon counting noise in the detector, as well as the dead time process. The resulting Fourier amplitudes will be of the form

$$\begin{aligned} A_{xj} &= A_{xsj} + A_{xdj} + A_{xnj} \\ B_{xj} &= B_{xsj} + B_{xdj} + B_{xnj} \, , \end{aligned} \tag{1}$$

where A_{xsj} and B_{xsj} denote the real and imaginary components of the signal power in the Fourier amplitudes, A_{xdj} and B_{xdj} denote the variance introduced by dead time, and A_{xnj} and B_{xnj} similarly denote the white noise components in the Fourier amplitudes. For a large enough number of data points N, the Fourier amplitudes A_{xj} and B_{xj} will be composed of a sum of three independent random normal variables, with $A_{xsj} \sim \mathcal{N}(0, \sigma_{sj}^2)$, $A_{xdj} \sim \mathcal{N}(0, \sigma_{dj}^2)$ and $A_{xnj} \sim \mathcal{N}(0, \sigma_n^2)$, where $\sigma_{sj}^2 = \sigma_s^2(\nu) = N_{\rm phot}P(\nu)/4$ is given by the (Leahy-normalized, Leahy et al. 1983) power spectrum of the underlying stochastic process, $P_j = P(\nu_j)$, σ_{dj}^2 is an unknown, frequency-dependent variance introduced by dead time, and $N_{\rm phot} = \sum_{k=1}^N x_k$ is the integrated flux in the light curve. We also have $\sigma_n^2 = N_{\rm phot}/2$, and hence the combined distributions become

$$\begin{aligned} A_{xj} &\sim \mathcal{N}(0, \sigma_{sj}^2 + \sigma_{dj}^2 + \sigma_n^2) \\ A_{yj} &\sim \mathcal{N}(0, \sigma_{sj}^2 + \sigma_{dj}^2 + \sigma_n^2) \, . \end{aligned}$$

Similar expressions can be found for A_{yj} and B_{yj}, respectively. It is important to note that $A_{xsj} = A_{ysj}$ and similarly $B_{xsj} = B_{ysj}$, that is, the amplitudes of the stationary noise process will be the same for the Fourier transforms of $\mathbf{x}$ and $\mathbf{y}$, while the components due to dead time and white noise differ between the two time series.

As depicted in Figure 1, the correlation between Fourier amplitudes implies that their difference will be independent of the source-induced variability $P(\nu_j)$ and will again be distributed following a normal distribution

$$A_{xj} - A_{yj} \sim \mathcal{N}(0, 2\sigma_{dj}^2 + 2\sigma_n^2) \, .$$

The difference in Fourier amplitudes effectively separates the frequency-dependent effects of source variability and variability due to detector effects.

4. DEAD TIME-AFFECTED WHITE NOISE

Let us simulate two constant light curves with an incident mean count rate of 400 counts/sec and a dead time of 2.5 ms, as we would expect from two identical detectors observing the same stable X-ray source (Figure 1, middle panel). The Fourier amplitudes A_{xj} and A_{yj} of the light curves from the two detectors are heavily distorted by dead time, with the characteristic damped oscillator-like shape (Vikhlinin et al. 1994; Zhang et al. 1995). As laid out in Section 3, the difference of Fourier amplitudes from two independent but identical detectors shows no source variability, but *still shows the same distortion* due to dead time. This gives a clear way to disentangle between source- and dead time-driven variability. By using the difference between the Fourier amplitudes in two detectors, we can in principle renormalize the power spectrum so that only the source variability alters its otherwise flat shape.

As shown in Figure 1 (right panel), the single-channel Fourier amplitudes are proportional to the difference of the Fourier amplitudes in different realizations, with a constant factor $1/\sqrt{2}$. Therefore, we expect that the periodogram will be proportional to the square of the Fourier amplitude difference, divided by 2. Let us try to *divide the power spectrum by a smoothed version of*

[4] https://github.com/matteobachetti/deadtime-paper-II

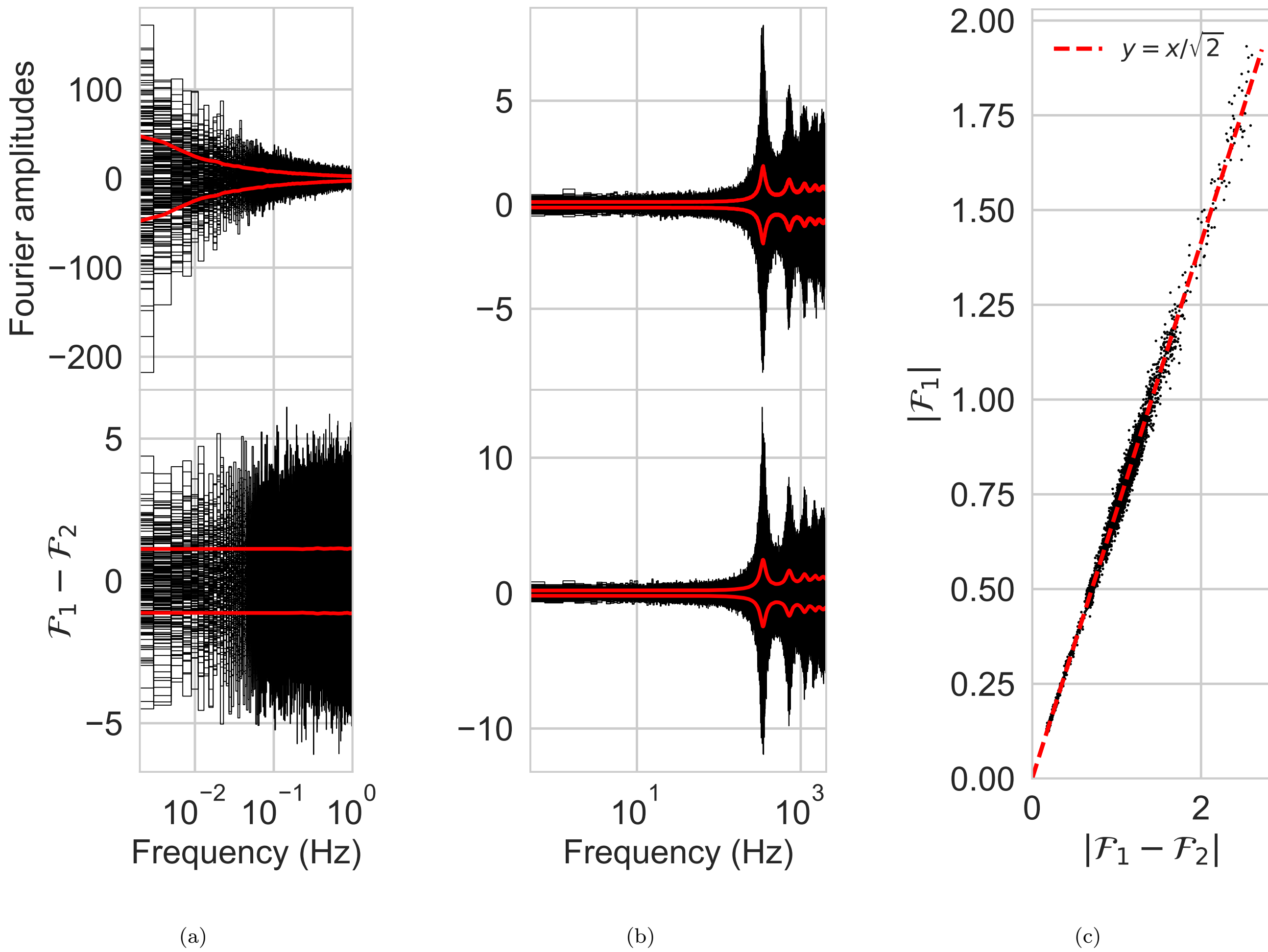

Figure 1. (a) and (b): Real-valued Fourier amplitudes obtained by single light curves (top panels) and difference between two realizations of the same source light curve (bottom) in two cases: (a) Strong $1/f$ red noise and no dead time, calculated over many 500 s segments of the light curve, and (b) no red noise and strong dead time, calculated over many 5 s segments of the light curve. The red curve gives the frequency-dependent spread of the distributions, measured by the mean of the absolute values of the curves in each frequency bin. The different behavior of Fourier amplitude differences under pure Poisson noise and dead time noise is evident, by comparing (a) and (b). (c) Scatter distribution of the absolute values of dead time-affected Fourier amplitudes versus the difference of Fourier amplitudes for case (b): their relation is clearly linear, with a factor $1/\sqrt{2}$.

the squared Fourier differences, and multiply by 2. For smoothing, we used a Gaussian running window with a window width of 50 bins. Given that the initial binning had 50 bins/Hz, this interpolation allows an aggressive smoothing over bins whose y value does not change significantly. We call this procedure the **Fourier Amplitude Difference** (hereafter FAD) **correction**.

The correction is depicted in Figure 2. Starting from a heavily distorted distribution of the powers, applying the FAD correction "flattens" remarkably well the white noise level of the periodogram and the distribution of the scatter of the white noise periodogram and cospectrum. Also, it reinstates a remarkably correct distribution of powers, following the expected χ^2_2 distribution (Lewin et al. 1988) very closely. Analogously, the corrected cospectrum will follow the expected Laplace distribution (**??**). While the original dead time-affected cospectrum had a frequency-dependent modification to the r.m.s. level, the FAD-corrected cospectrum gets back to a frequency-independent shape, like in the dead time-free case.

5. THE FAD CORRECTION ALGORITHM

In practice, the FAD correction algorithm in a generic case would work as follows:

1. split the two light curves in segments as one would do to calculate standard averaged periodograms;
2. for each pair of light curve segments:

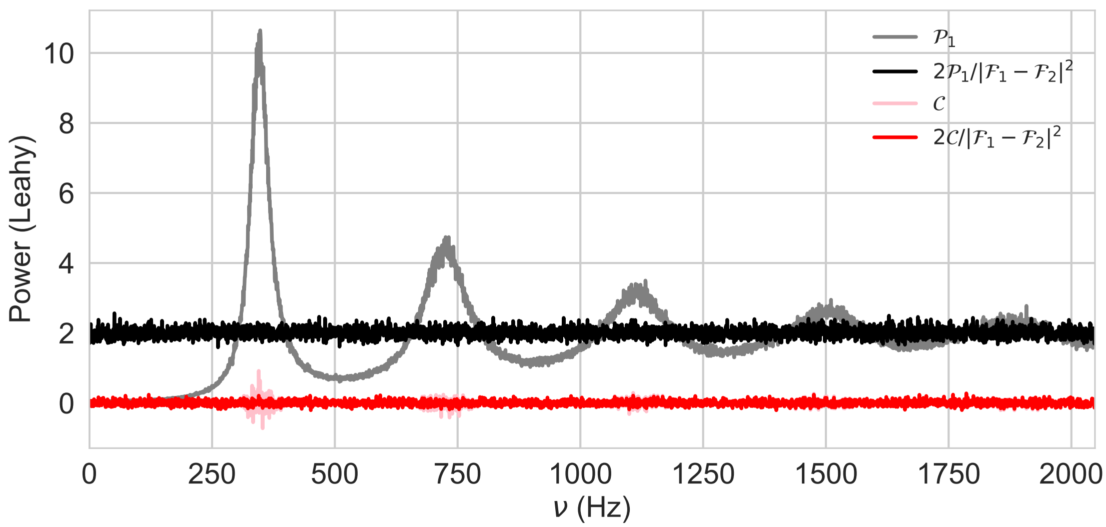

Figure 2. Periodogram and cospectrum, before and after FAD correction, for a pure white noise light curve. The deadtime-driven distortion of the white noise level in the periodogram, and the frequency-dependent modulation of the r.m.s. in both spectra, disappear after applying the FAD correction. Spectra were calculated over 2-sec intervals and averaged, to decrease the scatter and highlight the distortion of powers.

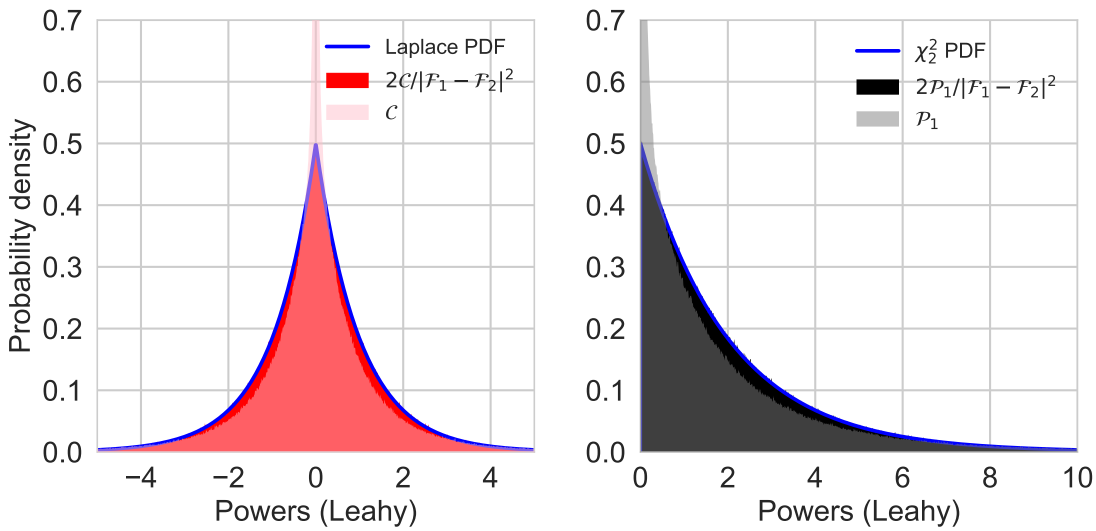

Figure 3. PDF of non-averaged powers in the cospectrum (red) and the periodogram (black), before the FAD correction and after, shown as a histogram. After correction, the powers follow remarkably well the expected Laplace and χ^2_2 distributions respectively, as highlighted by the overplotted probability density functions (PDF).

- calculate the Fourier transform of each channel separately, and then of the summed channels (hereafter total-intensity);
- save the unnormalized Fourier amplitudes;
- multiply these Fourier amplitudes by $\sqrt{2/N_{ph}}$ (that would give Leahy-normalized periodograms if squared);
- subtract the Leahy-normalized Fourier amplitudes of the two channels between them, *take the absolute value*, and obtain this way the Fourier Amplitude Differences (FAD);
- *smooth* the FAD using a Gaussian-window interpolation with a large number of bins, in our case all the bins contained in 1-2 Hz;

- use the separated single-channel and total-intensity *unnormalized* Fourier amplitudes to calculate the periodograms;
- use the unnormalized Fourier amplitudes from channels A and B to calculate the cospectrum;
- divide all periodograms and the cospectrum by the smoothed and squared FAD, and multiply by 2.

3. normalize the periodograms to the wanted normalization (Leahy or fractional r.m.s.).

6. TESTING THE FAD CORRECTION ON SIMULATED DATA

We are now ready to verify the last step: is the FAD-corrected power spectrum equivalent (albeit with some loss of sensitivity due to the lower number of photons) to the dead time-free power spectrum? To test this, we produced a number of different synthetic datasets as explained in Section 4, containing different combinations of QPOs and broadband noise components. We first calculated the periodogram and cospectrum of the dead time-free data, averaged over 128-s intervals. Then, we applied a dead time filter to the event list and applied the FAD correction, as described in Section 5

All spectra were then expressed in fractional r.m.s. (Belloni & Hasinger 1990; Miyamoto et al. 1991) normalization, where the integral of the fitted power spectral components over the frequency returns directly its fractional r.m.s.. In the r.m.s. normalization, the values of each point of the periodogram, after white noise subtraction, should be consistent between the dead time-free and the FAD-corrected periodograms. We fitted all spectra with the model which produced the simulated data and checked if the r.m.s. values were consistent with the fit on the dead time-free periodogram. To calculate this r.m.s., we fitted the spectra with two Lorentzian components, and integrated the model over the full frequency range. For periodograms, the model included also a constant offset to account for the white noise level. An example of this analysis is shown in Figure 4.

7. CAVEATS

The simulations show that the shape of the periodogram is precisely corrected by the FAD procedure *if the input light curves have the same count rate* and *for values of the input count rate and* r.m.s. *that are not too extreme*. The first caveat turns out to be an issue only for the single-channel periodogram. At high count rates, single-channel periodograms are corrected very well only if the two channels have very similar count rates, with the requirement being unsurprisingly stricter and stricter as the count rate increases. However, we find that the total-intensity periodogram and the cospectrum remains well corrected by the FAD even if the count rate in the two channels differs by 30%, for any reasonable count rate. Therefore, we recommend to use the FAD very carefully with single-channel periodograms, which should not be an issue given that the total-intensity periodogram is more sensitive and more convenient to use anyway. A comparison with the cospectrum, that is not affected by white noise distortions, is always recommended.

The second caveat needs some attention. We find that the FAD correction consistently overestimates the integrated r.m.s. when the count rate and r.m.s. are *both* very high, *in particular at low frequency* (See Figure 5). At standard count rates and fractional r.m.s. for bright black hole binaries, $\sim$200 ct/s and 30% r.m.s. for the *NuSTAR* case, the relative error is below 5% (meaning that if the r.m.s. is 30%, the measured r.m.s. is between 30 and 32%!) and it is symmetrically distributed around 0, as expected from statistical error. At higher incident rates and r.m.s., the error distribution skews towards positive relative errors, implying an overestimation of the r.m.s.. This should not be a problem in most cases, where the r.m.s. is used as a rough indicator for spectral state. If very precise measurements of r.m.s. are needed (for example, to calculate r.m.s./energy spectra), it is somewhat safer to account for this through simulations, without having to make further risky frequency-dependent corrections to the r.m.s.. As a rough estimate, the relative error on the fractional r.m.s. increases *linearly* with the count rate and *quadratically* with real r.m.s.. A practical way to estimate this effect during analysis is to apply the FAD, obtain a best fit model, calculate the r.m.s., then use the codes we shared with the Jupyter notebooks to simulate a number of realizations of the light curve, evaluating what is the amount of overestimation involved.

8. CONCLUSIONS

In this Letter we described a method to correct the normalization of dead time-affected periodograms. This method is valid in principle for 1) correcting the shape of the periodogram, eliminating the well known pattern produced by dead time, and 2) adjusting the white noise standard deviation of periodogram and cospectra to its correct value at all frequencies. In general, we recommend applying the FAD correction to both the periodogram and the cospectrum. The periodogram, if obtained by the sum of the light curves, can yield a higher

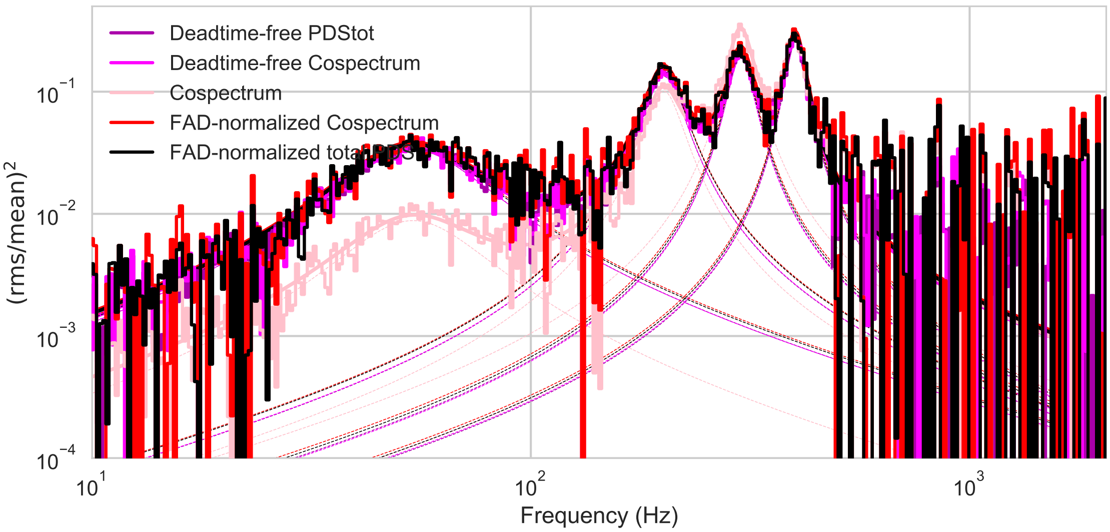

Figure 4. Periodograms and cospectra from a simulation with four Lorentzian features (at 50, 200, 300 and 400 Hz) with 40-Hz full with at half maximum (FWHM). We plotted and fitted periodograms and cospectra before and after applying the dead time filter The total r.m.s. before dead time was 40% and the incident photon flux 400 ct/s. After applying a dead time of 2.5 ms like in *NuSTAR*, the "detected" photon flux decreased to ∼200 ct/s as expected. As can be seen from the best-fit curves, there is no significant difference between FAD-normalized and deadtime-free periodograms and cospectra. For comparison, we also plot the cospectrum without FAD (pink), showing very different amplitudes for the four Lorentzians, due to dead time.

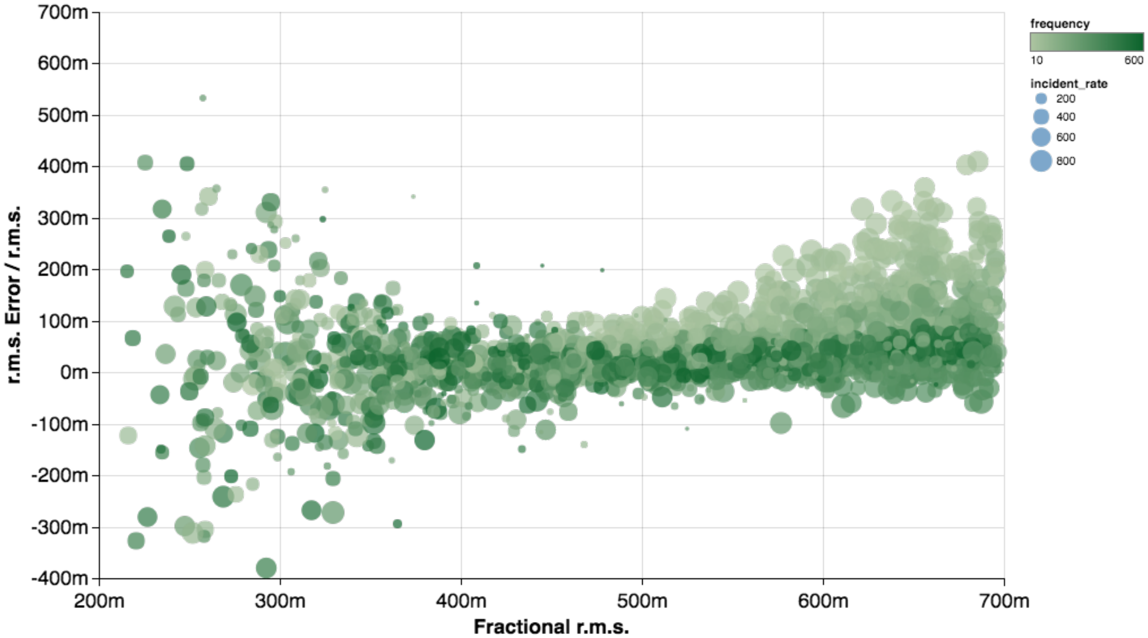

Figure 5. Relative overestimation of FAD with respect to r.m.s., versus r.m.s., as calculated from the cospectrum. We encoded the frequency of the feature in the color, and the incident rate in the size of the scatter points. From this visualization we see two regimes: below ∼40% fractional r.m.s., the errors are dominated by statistical errors. These errors will simply decrease when we average more data, as we expect from statistical errors. Over ∼40% fractional r.m.s., the errors are significantly skewed towards an overestimation of the r.m.s., and this is clearly truer when the incident rate *and* the r.m.s. are high.

signal-to-noise ratio. However, the white noise level subtraction is not always very precise due to mismatches in the mean count rate in the two light curves. A comparison with the FAD-corrected cospectrum, to verify visually the white noise subtraction, is always recommended. It is important to be reasonably sure of the white noise level of the periodogram, as the white noise subtraction is the most important step when calculating the significance of a given feature in the periodogram (e.g. Barret & Vaughan 2012; Huppenkothen et al. 2017). The cospectrum has the advantage of not requiring white noise level subtraction.

In all cases, we find that the adjustment of the white noise standard deviation in the periodogram and the cospectrum works remarkably well, allowing to make a confident analysis of X-ray variability even in sources where this was precluded until now. The only This software will be merged into the main repository of `stingray` before publication. A number of jupyter notebooks will also be posted at the address https://github.com/matteobachetti/deadtime-paper-II to reproduce the full analysis plotted in the Figures of this paper, plus more examples of application of these techniques to simulated and real data. The full algorithm described in Section 5 is contained in the `fad_correction.py` file in the notebooks directory, for reference.

We thank David W. Hogg for useful discussions on the topic of Fourier analysis. MB is supported in part by the Italian Space Agency through agreement ASI-INAF n.2017-12-H.0 and ASI-INFN agreement n.2017-13-H.0. DH is supported by the James Arthur Postdoctoral Fellowship and the Moore-Sloan Data Science Environment at New York University.

REFERENCES

Astropy Collaboration, Robitaille, T. P., Tollerud, E. J., et al. 2013, A&A, 558, A33

Bachetti, M. 2015, Astrophysics Source Code Library, ascl:1502.021

Bachetti, M., Harrison, F. A., Cook, R., et al. 2015, ApJ, 800, 109

Barret, D., & Vaughan, S. 2012, ApJ, 746, 131

Belloni, T., & Hasinger, G. 1990, A&A, 230, 103

Bowyer, S., Byram, E. T., Chubb, T. A., & Friedman, H. 1965, Astronomical Observations from Space Vehicles, 23, 227

Gilfanov, M., Churazov, E., & Revnivtsev, M. 2000, MNRAS, 316, 923

Grinberg, V., Hell, N., Pottschmidt, K., et al. 2013, 554, 88

Huppenkothen, D., Bachetti, M., Stevens, A. L., Migliari, S., & Balm, P. 2016, Stingray: Spectral-timing software, Astrophysics Source Code Library, , , ascl:1608.001

Huppenkothen, D., Younes, G., Ingram, A., et al. 2017, ApJ, 834, 90

Kluyver, T., Ragan-Kelley, B., Pérez, F., et al. 2016, in ELPUB, 87–90

Leahy, D. A., Darbro, W., Elsner, R. F., et al. 1983, ApJ, 266, 160

Lewin, W. H. G., van Paradijs, J., & van der Klis, M. 1988, SSRv, 46, 273

Miyamoto, S., Kimura, K., Kitamoto, S., Dotani, T., & Ebisawa, K. 1991, ApJ, 383, 784

Timmer, J., & Koenig, M. 1995, A&A, 300, 707

Vikhlinin, A., Churazov, E., & Gilfanov, M. 1994, 287, 73

Zhang, W., Jahoda, K., Swank, J. H., Morgan, E. H., & Giles, A. B. 1995, ApJ, 449, 930